Available online at www.sciencedirect.com
ScienceDirect
Catalysis Today 121 (2007) 255–260
www.elsevier.com/locate/cattod

Three primary kinetic characteristics observed in a pulse-response TAP experiment

S.O. Shekhtman *, N. Maguire, A. Goguet, R. Burch, C. Hardacre

CenTACat, School of Chemistry and Chemical Engineering, Queen's University, Belfast, David Keir Building, Stranmillis Road, Belfast BT9 5AG, Northern Ireland, UK

Abstract

The state-by-state transient screening approach based on a pulse-response thin-zone TAP experiment is further developed whereby single-pulse kinetic tests are treated as small perturbations to catalyst compositions and analyzed using integral method of moments. Results on three primary kinetic characteristics, termed basic kinetic coefficients, are presented. These three coefficients were introduced as main observables from experimentally measured TAP-responses in a kinetic-model-free manner. Each was analytically determined from moments of responses with no assumption about the detailed kinetic model. In this paper, the inverse question of how well these coefficients represent the time evolution of the observed responses is addressed. Sets of three basic kinetic coefficients are calculated from model and experimental responses and these calculated values are used to generate 3-coefficient curves in a kinetic-model-free manner. The comparison of these 3-coefficient curves with original responses shows that three basic kinetic coefficients can be sufficient to describe the observed kinetics of exit flow time dependencies with no assumption regarding the detailed kinetic model.

Keywords: Kinetics; Catalyst characterization; Pulse-response; Thin-zone; TAP-experiment; Primary kinetic characteristics

1. Introduction

The non-steady-state kinetic characterization of industrial multi-component catalysts has been a significant focus of heterogeneous catalytic research. The essential property of industrial catalytic systems is their complexity represented by three main, interwoven factors such as multi-component catalyst composition, complexity of the catalytic reaction itself and temporal change of the catalyst composition under the influence of the reaction medium. To overcome this complexity, a new theoretical and methodological approach for non-steady-state kinetic characterization of industrial catalysts, called state-by-state transient screening, was recently proposed [1–3]. The key idea of this approach is to kinetically test a catalyst with a particular composition (particular state of the catalyst) that does not change significantly during this transient test. A complete screening experiment includes a sequence of such tests performed over a catalyst with different compositions prepared separately and scaled, e.g. according to the reduction/oxidation scale. The approach is a combination of theoretical and experimental studies based on the following experimental principles:

(a) maintenance of a uniform chemical composition within the catalyst zone;
(b) insignificant catalyst change during a single transient experiment;
(c) control of reactant amount stored/released by the catalyst prior to each single transient experiment.

A simple single transient test can be considered a small perturbation because it does not change significantly the catalyst composition, which considerably decreases complexity of the system. Within this simplification, the efficient theory of integral analysis of small perturbations can generally be developed. For example, integrals (moments) of observed response can be used to calculate the primary kinetic characteristics with no assumption regarding the detailed kinetic model. Thereafter, a thorough understanding of the non-steady-state catalyst activity can be constructed in two steps:

---

* Corresponding author. Tel.: +44 28 9097 4882; fax: +44 28 9097 4687.
E-mail address: s.shekhtman@qub.ac.uk (S.O. Shekhtman).

0920-5861/$ – see front matter © 2006 Elsevier B.V. All rights reserved.
doi:10.1016/j.cattod.2006.08.068

Nomenclature

A_r	reactor cross-section area (cm^2)
C_{CS}	set of catalyst state concentrations (mole cm^{-3})
$C_g(x, t)$	set of gaseous concentrations (mole cm^{-3})
$C_\theta(x, t)$	set of surface concentrations (mole cm^{-3})
$\bar{C}_g$ and $\bar{C}_\theta$	gaseous and surface concentrations in the Laplace domain (mole cm^{-3} s^{-1})
D_{in} and D_{cat}	diffusivities in the inert and catalyst zones, respectively (cm^2 s^{-1})
$F(t, x)$	flow (mole s^{-1})
$\bar{F}_{exit}$	exit flow given in Laplace domain (mole s^{-2})
k_a	adsorption constant (s^{-1})
k_d	desorption constant (s^{-1})
k_r	reaction constant (s^{-1})
L_{in} and L_{cat}	lengths of the inert and catalyst zones, respectively (cm)
L_r	length of the whole reactor (cm)
M_n^i	nth order moment for ith probe molecule (mole s^n)
N_g	number of molecules in the inlet pulse (mole)
$r^{ij}(C_{CS}, s)$	Laplace reactivity that relates the rate for ith gas and jth gas concentration in the Laplace domain (s^{-1})
r_n^i	basic kinetic coefficient of nth order for ith probe molecule ($s^{(n-1)}$)
R, R_g	gas reaction rate (mole cm^{-3} s^{-1})
$\bar{R}_g$	gas reaction rate in Laplace domain (mole cm^{-3} s^{-2})
s	Laplace variable (s^{-1})
t	time coordinate (s)
x	space coordinate (cm)
X	conversion

Greek symbols

$\delta(t)$	dirac delta function
ε_{in} and ε_{cat}	bed voidages in the inert and catalyst zones, respectively
τ_{app}	apparent time delay (s)
$\tau_{cat} = L_r L_{cat}/2D_{in}$	residence time in the catalyst zone (s)
$\tau_{in} = \varepsilon_{in} L_r^2/2D_{in}$	residence time in inert zones (s)

I. a description with no preliminary assumption about the detailed kinetic model (“model-free” description) in terms of primary kinetic characteristics;
II. an analysis of these characteristics for different reactants/products as functions of catalyst composition (e.g. catalyst oxidation/reduction degree) and development of the detailed kinetic model.

The state-by-state transient screening approach can be generally realized using different experimental techniques. Originally, this approach was formulated based on the thin-zone modification of the TAP (temporal analysis of products) technique that has been successfully applied in many areas of chemical kinetics and chemical engineering [4,5], and has recently been reviewed [6]. The thin-zone TAP reactor (TZTR) was proposed by Shekhtman et al. [7] to insure uniformity in the catalyst zone (see also [8]) and has been shown, compared with other techniques, to be favorable for non-steady-state kinetic characterization of multi-component industrial catalysts [3] see also TZTR application in [9].

Within the developed TAP theory [1,2], three kinetic coefficients were introduced as primary kinetic characteristics measured in a TAP experiment. Appendix A provides the components of this theory that are relevant to the subject of this paper. In particular, a description as to how and on what ground these coefficients were introduced as primary kinetic characteristics of a single-pulse TAP experiment is provided. In addition, the general solutions for exit flows in the Laplace domain for different reactor configurations (A.5)–(A.7) and expressions for the basic kinetic coefficients as functions of moments (A.10)–(A.16) are presented.

Expressions (A.10) for the basic kinetic coefficients versus moments were derived with no assumption about detailed kinetic mechanism. Different mechanisms were considered and each coefficient, r_i, was expressed in terms of elementary reaction rate constants (see Table 1 in [1]). This provided the basis for identifying detailed kinetic mechanism from the observed basic kinetic coefficients.

Thus, the three basic kinetic coefficients can be used for characterizing the catalyst (as proposed above in bullet I) or distinguishing the mechanism (as proposed above in II). It should be noted however that these three coefficients are just a first part of Taylor approximation (A.9). Consequently, it is reasonable to ask how well these coefficients extract information about the observed kinetic process. This “inverse” question can be answered by determining how well these three coefficients can represent the time evolution of the observed TAP pulse-responses. In this paper we address this question.

2. Amount of information provided by the basic kinetic coefficients

According to expression (A.9), the basic kinetic coefficients determine Laplace reactivity as coefficients of Taylor expansion. Generally, there are an infinite number of these coefficients. Using solutions (A.5)–(A.7), the coefficients can be related to the exit flow moments, which also represent an infinite set of numbers. This is a mathematical picture. From experimental point of view, characteristics of importance are those that can be reliably measured (observed). Typically when moments of TAP pulse responses are analyzed, only first three moments (zeroth, first and second) can be reliably determined from the data. For this reason, only the first three basic kinetic coefficients were considered.

From this perspective, the moment analysis of one response curve provides three coefficients only, which together with Knudsen diffusivities describe the behavior of the whole response (a few thousand data points). This is different from the TAP data analysis when the shape of experimental response is fitted using a theoretical curve by varying many parameters of a detailed kinetic model.

In order to support the present approach, we studied a possibility to reproduce the model and experimental response curves from which the three basic kinetic coefficients were determined. It is especially interesting in terms of a model-free manner of the coefficient determination with which this paper is addressing.

3. Exact solution versus 3-coefficient curve

In this section we compare the exact solutions and responses generated from the three basic coefficients only. The following two-step model mechanism was considered:

$$A \underset{k_\mathrm{d}}{\overset{k_\mathrm{a}}{\rightleftarrows}} AZ, \quad AZ \xrightarrow{k_\mathrm{r}} B$$

The Laplace reactivity for this mechanism was determined as [2]:

$$r(s) = \frac{k_\mathrm{a}(k_\mathrm{r} + s)}{s + k_\mathrm{d} + k_\mathrm{r}} \qquad (1)$$

According to (A.9), this reactivity can be approximated using three basic kinetic coefficients as

$$r(s) \approx r_0 + r_1 s + r_2 s^2 = \frac{k_\mathrm{a} k_\mathrm{r}}{k_\mathrm{d} + k_\mathrm{r}} + \frac{k_\mathrm{a} k_\mathrm{d}}{(k_\mathrm{d} + k_\mathrm{r})^2} s - \frac{k_\mathrm{a} k_\mathrm{d}}{(k_\mathrm{d} + k_\mathrm{r})^3} s^2 \qquad (2)$$

Using reactivity expressions (1) and (2) together with TZTR solution (A.5), the exact (from (1)) and 3-coefficient (from (2)) curves were calculated by performing the back Laplace transformation of (A.5):

$$F_\mathrm{exit}(t) = \frac{1}{2\pi i} \int_{-\mathrm{i}\infty}^{+\mathrm{i}\infty} \mathrm{e}^{st} \bar{F}_\mathrm{exit}(s)\,\mathrm{d}s \qquad (3)$$

Values of varied parameters k_a, k_d and k_r as well as corresponding single-pulse conversion are summarized in Table 1. For all the calculations, two-characteristic diffusional times, τ_in and τ_cat were set at 0.1 and 0.01 s, respectively.

For each set of parameters, the exact curve (thick gray line) and 3-coefficient curve (thin black line) are plotted together versus time on two scales (Figs. 1 and 2 with non-zero conversion and Fig. 3 with zero conversion). All curves are normalized to the inlet pulse intensity. When k_d is high enough (Fig. 1), 3-coefficient curves perfectly reproduce exact solutions. When both k_d and k_r become relatively small (Fig. 2e and f), deviation of the 3-parameter curves from exact solution is observed in a short time region, i.e. <0.04 s. Similarly, when k_r is set to zero and only reversible adsorption occurs (Fig. 3), the 3-parameter curves deviates from exact solution at low values of k_d in a short time region, i.e. <0.08 s. In all cases, the 3-parameter curves reproduce exact solutions very well at middle and long t, i.e. >0.1 and 0.5 s, respectively.

Table 1
Values of parameters used for calculating curves plotted in Figs. 1–3

	Case	k_a (s^{-1})	k_d (s^{-1})	k_r (s^{-1})	X (%)
Fig. 1	(a)	500	500	10	8.9
Fig. 1	(b)	500	500	50	31.3
Fig. 1	(c)	500	500	100	45.5
Fig. 1	(d)	500	500	250	62.5
Fig. 1	(e)	500	500	500	71.4
Fig. 1	(f)	2000	500	500	90.9
Fig. 2	(a)	100	100	10	8.3
Fig. 2	(b)	100	100	50	25.0
Fig. 2	(c)	110	50	100	42.3
Fig. 2	(d)	150	20	100	55.6
Fig. 2	(e)	400	50	50	66.7
Fig. 2	(f)	500	20	50	78.1
Fig. 3	(a)	100	500	0	0
Fig. 3	(b)	500	500	0	0
Fig. 3	(c)	500	100	0	0
Fig. 3	(d)	500	50	0	0
Fig. 3	(e)	500	20	0	0

Deviation in the short time region has a simple, purely mathematical reason. The approximations (A.9) or (2) are parts of a Taylor series which may diverge at high s. For most of values of t, except short times in back Laplace transformation (3), the oscillating factor e^{ts} eliminates contribution from integrating over an interval with high absolute values of s. At small values of t, the factor e^{ts} does not oscillate frequently enough to eliminate contribution of high s. Consequently, whenever there is a problem with convergence of Taylor expansion, (A.9) or (2), it will influence the 3-parameter curve in the short time region. For the approximation in (2), the radius of Taylor series convergence is

$$\text{convergence radius} = k_\mathrm{d} + k_\mathrm{r} = \frac{1}{\tau_\mathrm{app}} \qquad (4)$$

Thus, when k_d and k_r are relatively small (τ_app is big), the 3-parameter curve may deviate from exact solution at small t. In

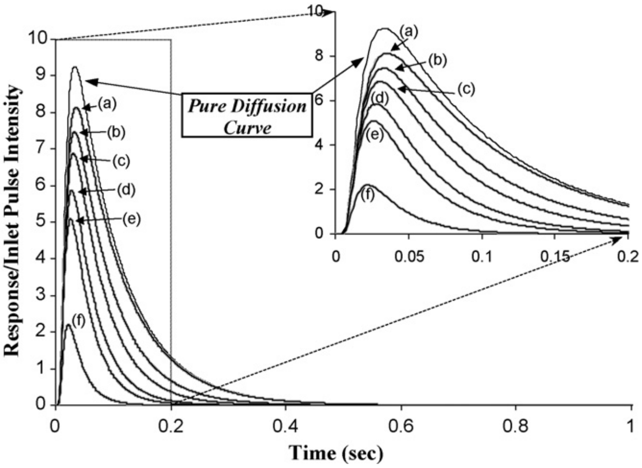

Fig. 1. Exact solutions (thick gray lines) and 3-coefficient approximations (thin black lines) plotted vs. time in two scales: 0–1 and 0–0.2 s. Parameters are given in Table 1.

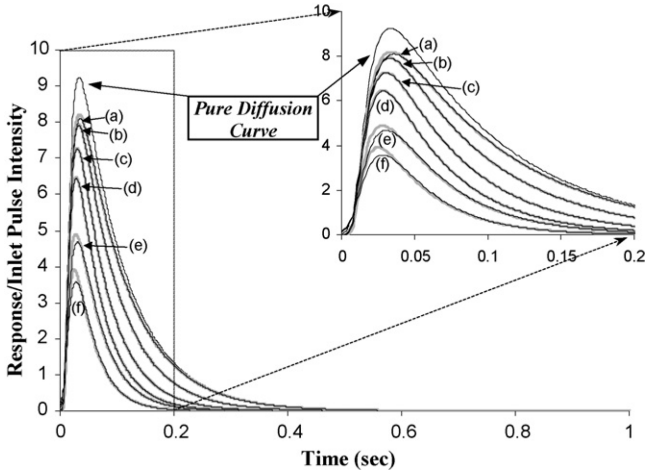

Fig. 2. Exact solutions (thick gray lines) and 3-coefficient approximations (thin black lines) plotted vs. time in two scales: 0–1 and 0–0.2 s. Parameters are given in Table 1.

general, the convergence radius of series (A.9) can be estimated as

$$\text{convergence radius} \approx \left|\frac{r_1}{r_2}\right| \equiv \frac{1}{\tau_{\text{app}}} \tag{5}$$

The deviation condition can be formulated by comparing τ_{app} and τ_{in}, e.g. such that τ_{app} is big enough to be of the same order or longer in magnitude than τ_{in}. The corresponding curve would be broad, with long middle and long time intervals where fit is already in good agreement.

It is important to stress that in general two time regions of TAP-response curves can be differentiated:

1. *Prior to the peak*. In this short time region, the response is contributed by fast molecules that happened to diffuse quickly through the reactor and not to interact with the catalyst. The shape is primarily determined by Knudsen diffusion.

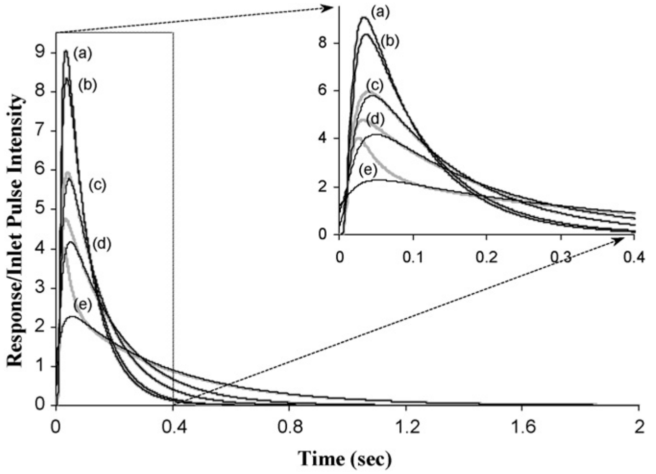

Fig. 3. Exact solutions (thick gray lines) and 3-coefficient approximations (thin black lines) plotted vs. time in two scales: 0–2 and 0–0.4 s. Parameters are given in Table 1.

Table 2
Values of parameters determined from the experimental responses and used for calculating 3-coefficient curves plotted in Fig. 4

Case	τ_{in} (s)	τ_{cat}	r_0 (s^{-1})	r_1	r_2 (s)	X (%)
(a)	0.094	0.013	107	2.29	0.181	66.8
(b)	0.094	0.013	28.5	0.66	0.039	34.9
(c)	0.094	0.013	8.23	0.21	0.025	13.4
(d)	0.094	0.013	1.87	0.18	0.019	3.4

2. *After the peak*. This region is usually the most informative because it is contributed by the slow ‘‘experienced’’ molecules that interact with the catalyst, get delayed by it instead of only diffusing towards the exit. The shape is influenced by both transport and reaction.

Thus, the deviation in the short time region is not critical. However, matching the exact solutions at middle and long *t* (the whole after peak region) means matching the kinetics observed in the experiment, which is the most important for TAP data analysis. Figs. 1–3 show that 3-coefficient curves are in good agreement at the point where the exact solution is most informative.

4. Experimentally observed response versus 3-coefficient curve

In this section we compare the experimentally observed responses and responses generated from the three basic coefficients. From each experimental response, the first three moments and then basic kinetic coefficients (r_0, r_1 and r_2) were obtained. The values of the coefficients were substituted into Taylor approximation (A.9) and then into solution (A.5). Finally, the 3-parameter curve was generated using the back Laplace transformation (3) of solution (A.5). The values of used parameters are given in Table 2.

Fig. 4 compares the CO responses observed in a multi-pulse TAP experiment over the 2 wt.%Au/CeZrO$_4$ catalyst at 200 °C with the corresponding 3-parameter approximation curves [10]. During the multi-pulse experiment, CO conversion decreased from 65% to 0. The experimental curves were normalized to the

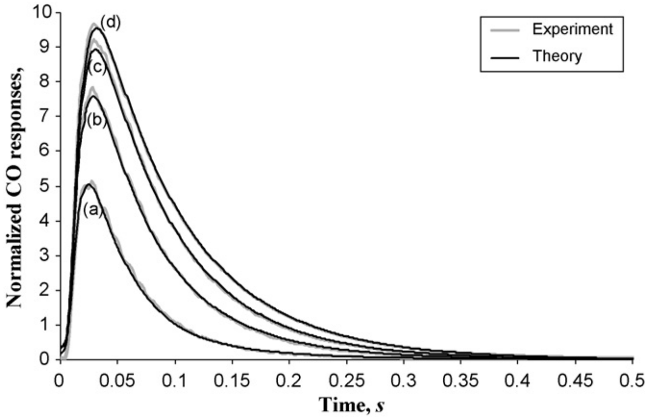

Fig. 4. CO responses observed in a multi-pulse TAP experiment over 2 wt.%Au/CeZrO$_4$ (thick gray lines) and 3-coefficient approximations (thin black lines): (a) 1–50 pulses averaged, (b) 101–150 pulses averaged, (c) 201–250 pulses averaged and (d) 1001–1100 pulses averaged.

amount of pulsed CO so that the area under the curve determines the conversion. As can be seen from Fig. 4, the 3-parameter curves are in a good agreement with corresponding experimental responses except in the region of very short times. Thus, the 3-parameter approximation is able to reproduce the major and most informative part of the experimental response. With regard to the short time region due to the divergence of the Taylor series in the Laplace domain, this difference needs to be treated mathematically and will be the subject of a further publication.

5. Conclusions

From the concept of state-by-state transient screening, three primary kinetic characteristics, termed basic kinetic coefficients, were introduced as observable from experimentally measured TAP-responses in a kinetic-model-free manner. It has been possible to show that the analytically determined coefficients from moments of responses with no assumption about the kinetic model can reproduce the observed experimental responses. This is achieved by initially calculating the three basic kinetic coefficients from model and experimental responses and then, using the calculated values, generating the 3-coefficient curves in a kinetic-model-free manner. The comparison of these 3-coefficient curves with original responses shows that three basic kinetic coefficients can be sufficient to describe exit flow time dependencies with no assumption regarding kinetic model.

Acknowledgements

We would like to thank Prof. G.S. Yablonsky and Dr. J.M. Yoda for many fruitful discussions. We acknowledge Johnson Matthey for supplying the catalyst, the EPSRC under the CARMAC project (SOS, AG) and the Department of Education in Northern Ireland (NM) for funding.

Appendix A. Mathematical background: general solution of TAP model, Laplace reactivity and basic kinetic coefficients

The general 3-zone model of a single-pulse TAP experiment that describes gas concentrations can be presented as [1]:

$$\varepsilon_{\text{in}} \frac{\partial C_{\text{g}}}{\partial t} = D_{\text{in}} \frac{\partial^2 C_{\text{g}}}{\partial x^2} \quad \text{in the inert zones} \tag{A.1}$$

$$\varepsilon_{\text{cat}} \frac{\partial C_{\text{g}}}{\partial t} = D_{\text{cat}} \frac{\partial^2 C_{\text{g}}}{\partial x^2} \pm R_{\text{g}}(C_{\text{g}}, C_\theta) \quad \text{in the catalyst zone} \tag{A.2}$$

Initial and boundary conditions: $C_{\text{g}}|_{t=0} = 0$, $C_{\text{g}}|_{x=L_{\text{r}}=2L_{\text{in}}+L_{\text{cat}}} = 0$, $-A_{\text{r}} D_{\text{in}} \frac{\partial C_{\text{g}}}{\partial x}\Big|_{x=0} = 2N_{\text{g}}\delta(t)$.

Here, the reaction rate, $R_{\text{g}}(C_{\text{g}}, C_\theta)$ is a function of gas and surface concentrations. This function depends on the detailed mechanism. To solve this TAP model in general (with no assumption about the mechanism), Shekhtman et al. [1] explored general kinetic properties of the single-pulse TAP experiment (the state-defining kinetic regime) in which a low intensity pulse of gas mixture changes a state of the catalyst insignificantly. The gas pulse can be considered a small perturbation described by the general theory of linear response. According to this theory, rates of all elementary processes are assumed to be linear with respect to the small perturbation that is a set of small gas or surface concentrations generated within a single-pulse experiment. Using this concept, all arbitrary surface concentrations were eliminated in general after transforming equations (A.1) and (A.2) into the Laplace domain. Then, reaction rates for gas substances were expressed as linear functions of gas concentrations in the Laplace domain with coefficients called Laplace reactivities [1,2]:

$$\bar{R}_i = \sum_j r^{ij}(C_{\text{CS}}, s)\bar{C}_j(s, x) \tag{A.3}$$

Laplace reactivities, $r^{ij}(C_{\text{CS}}, s)$, are components of a reactivity matrix that relates the rate vector (i index) to the gaseous concentration vector (j index) in the Laplace domain. The dimension of these reactivities is reciprocal seconds.

If only one reactant is involved in the pulse experiment and product generation is irreversible, for example during the oxidation of a hydrocarbon over the oxygen treated catalyst, the Laplace rates are linearly dependent on the reactant concentration:

$$\bar{R}_i = r^i(C_{\text{CS}}, s)\bar{C}_{\text{r}}(x, s) \tag{A.4}$$

Using linear "rate-concentration" expression (A.3) or (A.4), general TZ and 3-zone models were solved analytically in Laplace domain with no assumption about the detailed kinetic mechanism. The solutions are explicit expressions for the exit flow in the Laplace domain. In the single-reactant TZTR case, the reactant Laplace solution is [2]:

$$\bar{F}_{\text{exit}} = \frac{1}{\cosh(\sqrt{2s\tau_{\text{in}}}) + (r^{\text{r}}(C_{\text{CS}}, s)\tau_{\text{cat}}/\sqrt{2s\tau_{\text{in}}})\sinh(\sqrt{2s\tau_{\text{in}}})} \tag{A.5}$$

Correspondingly, the Laplace solution for the product exit flow was found as

$$\bar{F}_{\text{exit}} = \frac{\cosh(\sqrt{s\tau_{\text{in}} D^{\text{r}}_{\text{in}}/2D^{\text{p}}_{\text{in}}})\sinh(\sqrt{s\tau_{\text{in}}/2})\,(\sqrt{2}r^{\text{p}}(C_{\text{CS}}, s)\tau_{\text{cat}}/\sqrt{s\tau_{\text{in}}})}{(\cosh(\sqrt{2s\tau_{\text{in}}}) + (r^{\text{r}}(C_{\text{CS}}, s)\tau_{\text{cat}}/\sqrt{2s\tau_{\text{in}}})\sinh(\sqrt{2s\tau_{\text{in}}}))\cosh(\sqrt{2s\tau_{\text{in}} D^{\text{r}}_{\text{in}}/D^{\text{p}}_{\text{in}}})} \tag{A.6}$$

In addition, the reactant exit flow in the Laplace domain was calculated for the symmetric 3-zone reactor configuration:

$$\bar{F}_{\text{exit}} = \frac{1}{\begin{aligned}&(\cosh(L_{\text{cat}}\sqrt{r^{\text{r}}(C_{\text{CS}}, s) + s\varepsilon_{\text{cat}}}/\sqrt{D^{\text{r}}_{\text{cat}}})\cosh(2L_{\text{in}}\sqrt{s\varepsilon_{\text{in}}}/\sqrt{D^{\text{r}}_{\text{in}}}) + \sinh(L_{\text{cat}}\sqrt{r^{\text{r}}(C_{\text{CS}}, s) + s\varepsilon_{\text{cat}}}/\sqrt{D^{\text{r}}_{\text{cat}}})\\ &\sinh(2L_{\text{in}}\sqrt{s\varepsilon_{\text{in}}}/\sqrt{D^{\text{r}}_{\text{in}}})(D^{\text{r}}_{\text{cat}}(r^{\text{r}}(C_{\text{CS}}, s) + s\varepsilon_{\text{cat}}) + D^{\text{r}}_{\text{in}}s\varepsilon_{\text{in}})/2\sqrt{D^{\text{r}}_{\text{cat}}(r^{\text{r}}(C_{\text{CS}}, s) + s\varepsilon_{\text{cat}})D^{\text{r}}_{\text{in}}s\varepsilon_{\text{in}}})\end{aligned}} \tag{A.7}$$

In solutions (A.5)–(A.7), the reaction kinetics is described using Laplace reactivities, $r^{\mathrm{r}}(C_{\mathrm{CS}}, s)$ for the reactant and $r^{\mathrm{p}}(C_{\mathrm{CS}}, s)$ for the product, which are functions of the catalyst state concentrations, C_{CS}, and Laplace variable, s.

Purely mathematical Laplace solutions (A.5)–(A.7) were linked to the experimentally observed exit flow time dependencies using the moment technique [11]. The exit flow moments, M_n, can be obtained from the exit flow Laplace solution, $\bar{F}_{\mathrm{exit}}$, as

$$M_n = \int_0^{+\infty} t^n F_{\mathrm{exit}}(t)\,\mathrm{d}t = (-1)^n \left.\frac{\partial^n \bar{F}_{\mathrm{exit}}(s)}{\partial s^n}\right|_{s=0} \tag{A.8}$$

In this expression, the derivatives with respect to the variable s at $s = 0$ suggested the following Taylor series approximation for the Laplace reactivity:

$$r^i(C_{\mathrm{CS}}, s) = r_0^i(C_{\mathrm{CS}}) + r_1^i(C_{\mathrm{CS}})s + r_2^i(C_{\mathrm{CS}})s^2 + O(s^3) \tag{A.9}$$

where the constants, $r_n^i(C_{\mathrm{CS}})$, were termed the basic kinetic coefficients for a specific probe molecule (i) and particular catalyst state.

Using expressions (A.8) and (A.9) and solutions (A.5)–(A.7), the basic kinetic coefficients were analytically related to the moments of the exit flows for TZ and 3-zone models [1,2]. In general, they can be presented as

$$\begin{aligned} r_0 &= f_0\,(M_0, \text{Knudsen Transport}),\\ r_1 &= f_1(M_1, M_0, \text{Knudsen Transport}),\\ r_2 &= f_2(M_2, M_1, M_0, \text{Knudsen Transport}) \end{aligned} \tag{A.10}$$

The explicit forms of functions f_1, f_2 and f_3 for the 3-zone packing can be derived from [1,2]. For the TZTR, these functions are relatively simple and can be reported here. For a reactant (r) they are

$$r_0^{\mathrm{r}} = \frac{1 - M_0^{\mathrm{r}}}{\tau_{\mathrm{cat}} M_0^{\mathrm{r}}} \tag{A.11}$$

$$r_1^{\mathrm{r}} = \frac{M_1^{\mathrm{r}}}{\tau_{\mathrm{cat}} {M_0^{\mathrm{r}}}^2} - \tau_{\mathrm{in}}\left(\frac{1}{\tau_{\mathrm{cat}}} + \frac{r_0^{\mathrm{r}}}{3}\right) \tag{A.12}$$

$$-r_2^{\mathrm{r}} = \frac{M_2^{\mathrm{r}}}{2\tau_{\mathrm{cat}} {M_0^{\mathrm{r}}}^2} - \frac{{M_1^{\mathrm{r}}}^2}{\tau_{\mathrm{cat}} {M_0^{\mathrm{r}}}^3} + \frac{\tau_{\mathrm{in}}}{6}\left(\frac{\tau_{\mathrm{in}} r_0^{\mathrm{r}}}{5} + 2r_1^{\mathrm{r}} + \frac{\tau_{\mathrm{in}}}{\tau_{\mathrm{cat}}}\right) \tag{A.13}$$

And for products (p):

$$r_0^{\mathrm{p}} = \frac{M_0^{\mathrm{p}}}{\tau_{\mathrm{cat}} M_0^{\mathrm{r}}} \tag{A.14}$$

$$-r_1^{\mathrm{p}} = r_0^{\mathrm{p}}\left[\frac{M_1^{\mathrm{p}}}{M_0^{\mathrm{p}}} - \frac{\tau_{\mathrm{in}}}{12}\left(8M_0^{\mathrm{r}} + 3 + 9\frac{D_{\mathrm{in}}^{\mathrm{r}}}{D_{\mathrm{in}}^{\mathrm{p}}}\right) - \tau_{\mathrm{cat}} M_0^{\mathrm{r}} r_1^{\mathrm{r}}\right] \tag{A.15}$$

$$\begin{aligned} r_2^{\mathrm{p}} = \frac{r_0^{\mathrm{p}}}{2}\Bigg(&\frac{M_2^{\mathrm{p}}}{M_0^{\mathrm{p}}} - \frac{19{D_{\mathrm{in}}^{\mathrm{r}}}^2 \tau_{\mathrm{in}}^2}{16{D_{\mathrm{in}}^{\mathrm{p}}}^2} - \frac{\tau_{\mathrm{in}} D_{\mathrm{in}}^{\mathrm{r}}}{8D_{\mathrm{in}}^{\mathrm{p}}}\\ &\times\left((3 + 8M_0^{\mathrm{r}})\tau_{\mathrm{in}} + 12M_0^{\mathrm{r}} r_1^{\mathrm{r}} \tau_{\mathrm{cat}} - 12\frac{r_1^{\mathrm{p}}}{r_0^{\mathrm{p}}}\right)\\ &- \frac{1}{6}M_0^{\mathrm{r}}(3 + 16M_0^{\mathrm{r}}) r_1^{\mathrm{r}} \tau_{\mathrm{in}} \tau_{\mathrm{cat}} - 2M_0^{\mathrm{r}} \tau_{\mathrm{cat}}(M_0^{\mathrm{r}} {r_1^{\mathrm{r}}}^2 \tau_{\mathrm{cat}} - r_2^{\mathrm{r}})\\ &+ \frac{r_1^{\mathrm{p}}}{6r_0^{\mathrm{p}}}((3 + 8M_0^{\mathrm{r}})\tau_{\mathrm{in}} + 12M_0^{\mathrm{r}} r_1^{\mathrm{r}} \tau_{\mathrm{cat}})\\ &- \tau_{\mathrm{in}}^2\left(\frac{5}{48} + \frac{1}{45}M_0^{\mathrm{r}}(23 + 40M_0^{\mathrm{r}})\right)\Bigg) \end{aligned} \tag{A.16}$$

Using (A.10)–(A.16), the basic kinetic coefficients can be unambiguously calculated one after another from the moments of the experimentally observed exit flow. This is why the coefficients were introduced as *primary kinetic characteristics* measured in a TAP experiment with no assumption about detailed kinetic mechanism. Their physico-chemical meaning was understood as:

- The zeroth coefficient, r_0, has the dimension of reciprocal time (seconds) and represents an apparent kinetic constant for the chemical transformation of a given gaseous substance.
- The first coefficient, r_1, is dimensionless and represents an apparent "intermediate-gas" constant of the catalyst for a given gaseous substance, which relates gas substances with preceding intermediates.
- The second coefficient, r_2, has the dimension of time (s) and describes an apparent time delay caused by processes on or in the solid material.

References

[1] S.O. Shekhtman, G.S. Yablonsky, J.T. Gleaves, R. Fushimi, Chem. Eng. Sci. 58 (2003) 4843–4859.

[2] S.O. Shekhtman, Interrogative kinetics, A new methodology for catalyst characterization, PhD dissertation, Washington University in St. Louis, 2003.

[3] S.O. Shekhtman, G.S. Yablonsky, J.T. Gleaves, R. Fushimi, Chem. Eng. Sci. 59 (2004) 5493–5500.

[4] J.T. Gleaves, J.R. Ebner, T.C. Kuechler, Catal. Rev. Sci. Eng. 30 (1988) 49–116.

[5] J.T. Gleaves, G.S. Yablonskii, Ph. Phanawadee, Y. Schuurman, Appl. Catal. A: Gen. 160 (1997) 55–87.

[6] G.S. Yablonsky, M. Olea, G.B. Marin, J. Catal. 216 (2003) 120–134.

[7] S.O. Shekhtman, G.S. Yablonsky, J.T. Gleaves, S. Chen, Chem. Eng. Sci. 54 (1999) 4371–4378.

[8] P. Phanawadee, S.O. Shekhtman, C. Jarungmanorom, G.S. Yablonsky, J.T. Gleaves, Chem. Eng. Sci. 58 (2003) 2215–2227.

[9] A. Goguet, S.O. Shekhtman, R. Burch, C. Hardacre, F.C. Meunier, G.S. Yablonsky, J. Catal. 237 (2006) 102–110.

[10] The catalyst was prepared as described in.
D. Tibiletti, A. Amieiro-Fonseca, R. Burch, Y. Chen, J.M. Fisher, A. Goguet, C. Hardacre, P. Hu, D. Thompsett, J. Phys. Chem. 109 (2005) 22553–22559.

[11] G.S. Yablonskii, S.O. Shekhtman, S. Chen, J.T. Gleaves, Ind. Eng. Chem. Res. 37 (1998) 2193–2202.